

MODELLING AND EXPERIMENTS OF SOLIDIFICATION OF AISI 304

D. Baldissin, M. Palumbo, L. Battezzati

In the first part of this paper the solidification of AISI 304 is simulated by means of the multicomponent phase selection theory to predict which phase forms first when the molten alloy is solidified either δ or γ .

The eventual δ - γ transition that may occur in AISI 304-type steels has influence on cracking tendency being increased at high solidification velocities.

It has been shown that alloys solidified as primary ferrite are more resistant to cracking than those solidified as primary austenite. In the second part of the paper solidification experiments have been performed at high cooling rates by using copper mould casting technique.

By means of this technique, it has been possible to reproduce microstructures usually obtained in industrial processes such as welding.

Finally, in the last part of the paper multicomponent diffusion theory has been used in order to treat the moving boundary problem in solidification and describe microsegregation phenomena.

KEYWORDS: solidification, steel, multicomponent phase selection theory, multicomponent diffusion theory, microsegregation

INTRODUCTION

One of the most important processes in material science, especially for metals and alloys, is solidification. Over the last decades much progress has been made in understanding this complex phenomenon in order to control those processing parameters influencing uniformity in microstructure.

Solidification behaviour depends on the evolution of the interface in time and controls the size and shape of grains, the extent of segregation, the distribution of inclusions, the extent of defects such as porosity and hot cracks. During growth any interface will be subject to random disturbances caused by insoluble particles, temperature fluctuations or grain boundaries. The main difficulty in the development of a growth model is caused by the geometry of the system. The more the geometry is complex the more differential equations

underlying solidification process become difficult to solve. Therefore, analytical models have been substituted with numerical models that have led to important advances in solidification science [1-5].

Nowadays, numerical techniques allow to handle problems regarding interface dynamics, phase selection, microstructure selection, peritectic growth, convection effects, multicomponent alloy, rapid solidification, taking into account not only steady state (typical problem of analytical models) but also non-steady state phenomena.

Part of the theoretical results have been possible thanks to the use of powerful trademark software like THERMO-CALC, DICTRA and MATLAB.

The central target of this work has been the development of a general multi-component model that, differently from CDG (based upon a database designed only for AISI 304-like steels), could be valid for any alloy once the thermo-physical properties of the system are known.

Further information are also derived from microsegregation modelling [6-8]. The compositional variations or coring on the scale of dendrite arms can be caused by the redistribution of solute during solidification, as

D. Baldissin, M. Palumbo, L. Battezzati

Dipartimento di Chimica I.F.M.,

Centro di Eccellenza Superficie d'Interfasi Nanostrutturate (NIS),
Università di Torino, Torino, Italy

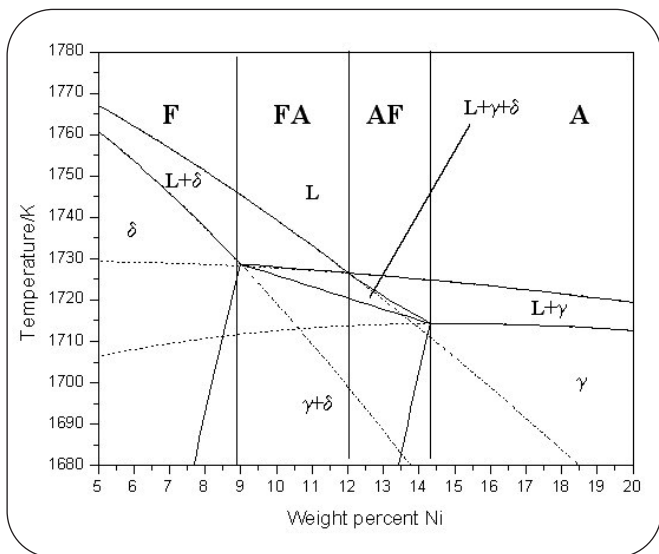


Fig. 1

Vertical section of Fe-Ni-Cr ternary diagram calculated with the Thermocalc software, at constant Fe content (72 wt-%). Dashed and dot dashed lines represent liquidus lines extrapolated at temperatures lower than the equilibrium liquidus.

Sezione verticale del diagramma ternario Fe-Ni-Cr calcolato con il software Thermocalc al 72 wt-% Fe. Le linee tratteggiate e puntate rappresentano le linee di liquidus estrapolate a temperature più basse delle liquidus di equilibrio.

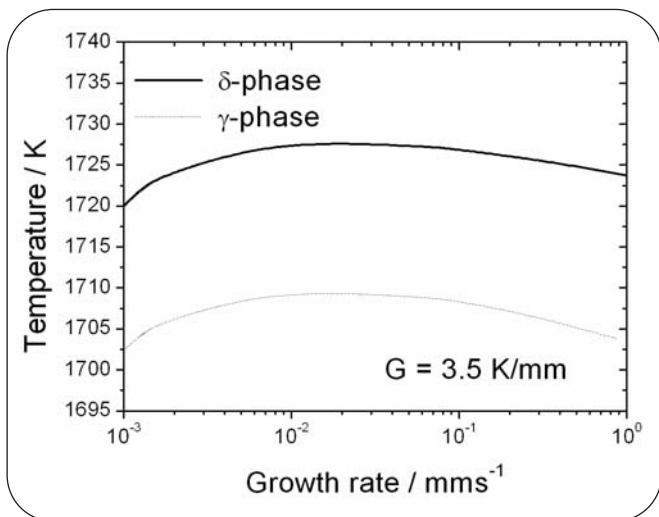


Fig. 2

Dendrite tip temperature for δ and γ phases as a function of the growth rate calculated using the multicomponent model.

Temperatura della punta dendritica per la fase δ e γ in funzione della velocità di crescita calcolata usando il modello a molti componenti.

solute is generally rejected into the liquid. The compositional gradients of solute extend on a micron scale and they can cause the formation of a second phase or porosity. Part of the results obtained from the simula-

tion with DICTRA and the phase selection theory have been verified experimentally by means of rapid solidification experiments.

Solidification modes and phase selection theory Fe-Ni-Cr is the base system for stainless steels, where the concentration of Cr must be higher than 18%. Assessed databases are available for the ternary system [9] and pseudobinary phase diagram can be calculated. A section of the ternary stable and metastable phase diagrams, calculated for a fixed Cr content of 18 wt%, is reported in Fig. 1, which refers to compositions close to the boundary between ferritic and austenitic stainless steels. Continuous lines correspond to the stable phase diagram, whereas dashed and dotted-dashed lines correspond to metastable phase diagram, obtained by suspending the bcc (ferrite) and the fcc (austenite) solid solutions, respectively. Equilibrium solidification paths for stainless steel may be summarised as follow [10]:

Mode A: $L \rightarrow (L + \gamma) \rightarrow \gamma$

$(Cr_{eq}/Ni_{eq}) < 1.25$

Mode AF: $L \rightarrow (L + \gamma) \rightarrow (L + \gamma + \delta) \rightarrow (\gamma + \delta)$

$1.25 < (Cr_{eq}/Ni_{eq}) < 1.48$

Mode FA: $L \rightarrow (L + \delta) \rightarrow (L + \delta + \gamma) \rightarrow (\delta + \gamma)$

$1.48 < (Cr_{eq}/Ni_{eq}) < 1.95$

Mode F: $L \rightarrow (L + \delta) \rightarrow \delta \rightarrow (\gamma + \delta)$

$(Cr_{eq}/Ni_{eq}) > 1.95$

where L is the liquid and δ and γ represent ferrite and austenite phases, respectively, as schematically shown in Fig. 1. In solidification modes F and FA the equilibrium primary phase is ferrite, while in modes A and AF the primary phase is austenite. Solidification paths may be modified as a function of cooling rate. This is demonstrated by the theory of undercooling at the dendrite tip which states that the phase favoured in growth is the one having the higher temperature at the interface [11-12].

In fact, when compositions corresponding to modes F and FA are solidified at high cooling rates, some undercooling of the liquid may promote the nucleation of metastable austenite instead of stable ferrite. In addition, as a consequence of the high solidification rates, short diffusion distance are involved, leading to fine and homogeneous microstructures. Both effects appear suitable for a significant improvement of mechanical properties of the material. From the analysis of stable and metastable phase diagrams shown in Fig. 1, it is apparent that, in order to have a driving force for nucleation of austenite, a larger undercooling is necessary for compositions giving solidification mode F with respect to those giving solidification mode FA.

For instance, an alloy containing 8.5 wt% Ni (mode F) must be undercooled of about 20 K, in order to reach the metastable liquidus curve for the austenite, whereas for an alloy containing 11 wt% Ni (mode FA) an undercooling of about 5 K is sufficient. In rapid solidification of steels with higher Ni content (mode AF) the formation of ferrite occurs in undercooling conditions, so that austenite is produced from solid state transformation, reducing volume contraction and surface cracks formation [13]. For this reason, the control of the δ - γ transition typical for these steels which occurs on cooling in the solid state is of fundamental importance for the quality of cast products [14-15]. A further increase of Ni content in the steel gives solidification mode A, so that

Cr (wt.%)	Ni (wt.%)	Mn (wt.%)	C (wt.%)	Cu (wt.%)	Si (wt.%)	Mo (wt.%)
18.3	8.1	1.4	0.047	0.28	0.29	0.11

▲
Tab. 1

Composition of the steel used in simulation and in the experiments.

Composizione dell'acciaio usata nella simulazione e negli esperimenti.

austenite is formed directly from the melt with a primary reaction.

The understanding of the mechanism of solidification will provide information on the sequence of phase formation and allows to predict whether the ferrite content will increase or decrease with cooling rate. In fact, the cooling rate influences both the amount of primary dendritic ferrite that solidifies from the liquid and the amount of ferrite due to the transformation to austenite during cooling to room temperature. The residual ferrite content of alloys that solidify as primary ferrite can increase when the cooling rate increases because at high rates a reduced amount of δ - γ transformation occurs. On the contrary, alloys that solidify as primary dendritic austenite and form δ as secondary phase, have decreasing ferrite content when the cooling rate increases because less ferrite forms during solidification at high rates [16].

MULTICOMPONENT PHASE SELECTION THEORY

Usually phase selection models found in the literature for steels [17-19], predict the solidifying primary phase with reference to the Fe-Cr-Ni ternary by using the concept of equivalents [20-21].

However, the reduction of a multicomponent steel to the simple Fe-Cr-Ni ternary may lead to wrong predictions because the effect of the various solutes is approximately parametrized [22]. The composition of the steel used in our model is given in Tab. 1. The weight percent of each element is in the range foreseen by the database TCFE_2000 of THERMO-CALC.

In this paper the phase selection model is extended to multicomponent systems in order to take the effect of solutes into account to calculate the dendrite tip temperature as a function of the growth rate for both γ and δ phases. The first models of growth proposed by Ivantsov et al. [23] predicted a multiplicity of possible solutions owing to the fact that the product of the radius R of the dendrite tip with the growth rate V was constant. By a physical point of view the fact that VR is constant means that a dendrite with a small radius will grow rapidly while a dendrite with a large radius will grow slowly. Such a criterion is called "growth criterion at extremus" but it disagreed with experimental results. Langer and Müller-Krumbhaar [24] proposed to use a new criterion named "marginal stability criterion" that states that the radius of curvature of the dendrite is close to the lowest wavelength perturbation of the tip. Therefore the relation $VR = \text{const.}$ is substituted with the relation $VR^2 = \text{const.}$ and doing so the multiplicity of the possible solution is removed [25].

Taking into account the marginal stability criterion extended to a multicomponent system [26-27] the theo-

ry of free dendritic growth leads to the following equation for the calculation is known:

$$R = \frac{\Gamma / \sigma^*}{Pe_i \frac{\Delta H_f}{C_p} (1-j) - \sum_{i=1}^n \frac{2Pe_i m_i C_{0,i} (1-k_i)}{1 - (1-k_i) \text{Ivan}(Pe_i) (1-g_i)} \quad (1)$$

where ΔH_f is the latent heat, C_p is the specific heat, σ^* is the Gibbs-Thompson coefficient, m is the liquidus slope, D is the diffusion coefficient in the liquid, k is the partition coefficient, Pe_i is the thermal Peclet number, Pe_i is the solute Peclet number while the index "i" refers to the various solutes. The denominator of eq. (1) represents the difference between the gradient due to the thermal field and that due to the solute field. Such a difference is always positive in an undercooled melt and its destabilizing effect is balanced by the stabilizing effect of the capillarity term σ^* / σ^* [28]. The interfacial energy σ is one of the most critical parameters in solidification modeling owing to the difficulty to measure it experimentally. It is defined as:

$$\Gamma = \frac{\sigma}{\Delta s_f} \quad (2)$$

Arnold et al. [29] addressed the calculation of σ (the interface energy) based on the model of Spaepen [30]. Spaepen's model relates the σ to ΔS_i (entropy change) and type of crystal structure for monoatomic system. Moreover the following quantities of equation (1) are defined as follows:

$$j = \frac{1}{\sqrt{1 + (1/\sigma^* Pe_i^2)}} \quad (3)$$

$$g_i = \frac{2k_i}{1 - 2k_i - \sqrt{1 + (1/\sigma^* Pe_i^2)}} \quad (4)$$

Equation (1) has been solved numerically by using a code written in MATLAB language. In the calculations the Gauss-Newton and Levenberg-Marquardt methods based on the nonlinear least-squares algorithms have been used [31].

By means of THERMO-CALC it has been possible to calculate the parameters needed for the development of the model: the liquidus temperature, the latent heat of fusion and the solidification range. Input parameters are reported in Tab. 2. The Gibbs-Thompson coefficients have been taken from the literature [32-33].

Other important parameters are the activation energies and the pre-exponential diffusion coefficients in the liquid and in the two solid phases δ and γ for each solute element. These data have been extracted from [34].

Once V and R are known the growth temperature is obtained by means of the following explicit expression for the undercooling:

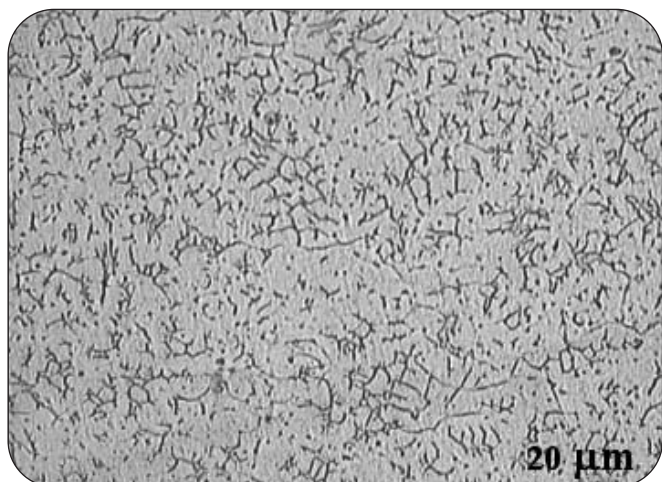


Fig. 3

Skeletal type or vermicular microstructure in a copper moulded cone of AISI 304. This type of microstructure is due to low undercoolings typical of the base of the cone.

Microstruttura di tipo scheletrico o vermicolare di una sezione di un cono di AISI 304 ottenuto dalla colata in stampo di rame. Questo tipo di microstruttura è dovuta ai bassi sottoraffreddamenti riscontrati alla base del cono.

$$T_i = T_m + \sum_i m_i C_{i,s} - 2\Gamma / R - GD/V \quad (5)$$

where $C_{i,s}$ is the composition of the tip for each solute i . The result of the calculation is shown in Fig. 2 where the dendrite tip temperature for both γ and δ phases is reported as a function of the growth rate. No transition from δ to γ occurs since the dendrite tip temperature of the δ phase is always higher than that of the γ phase. Therefore, in the range of the growth rates considered in Fig. 2 the non-equilibrium solidification mode predicts first the formation of ferrite followed by the formation of austenite. Higher growth rates lead to the formation of primary austenite directly from the liquid. The dendritic growth model is not valid at these high growth rates because the planar front becomes stable and the absolute stability limit, of the order of 102 mm/s, is exceeded.

EXPERIMENTAL RESULTS

Thermophysical properties	Ferrite	Austenite
$T_{\text{liquidus}} \text{ (K)}$	1730	1712
$\Delta H \text{ (J/mol)}$	11425.2	12080.1
$\Delta T_{\text{sol/liq}} \text{ (K)}$	43.5	32
$\Delta \text{ (mK)}$	$2.18 \cdot 10^7$	$2.89 \cdot 10^7$ [29-30]

Tab. 2

Thermophysical properties calculated for the composition of the steel used in the model.

Proprietà termofisiche calcolate per la composizione dell'acciaio usata nel modello.

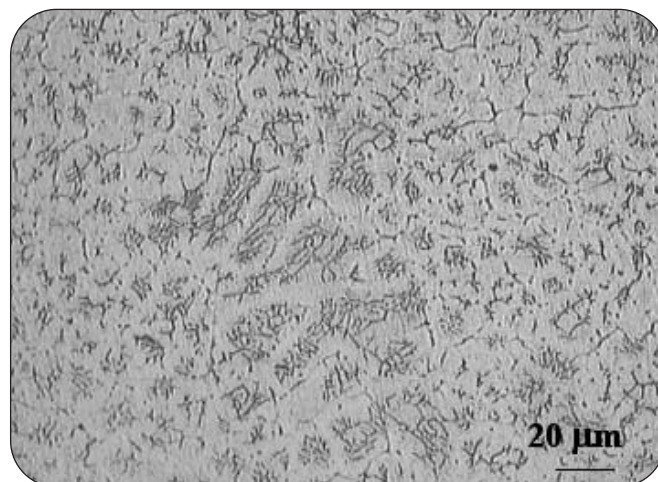


Fig. 4

Skeletal microstructure with lathy ferrite in the cone of AISI 304 (0.5 cm from the base).

Microstruttura scheletrica con ferrite "lathy" nel cono di AISI 304 (0.5 cm dalla base).

To simulate rapid solidification processes we used casting into a copper conic mould as a laboratory technique. Samples were cast into a copper conic mould, 20 mm in height and 4 mm in base radius. Transverse and longitudinal cross sections have been cut in order to investigate the microstructures (etching solution 5g FeCl₃, 100 ml HCl and 300 ml distilled water). The specimens were observed with optical microscopy and scanning electron microscopy. X-ray diffraction has been performed by using Co K α radiation.

The samples of different thicknesses experienced various cooling rates. The related microstructures can be representative of stages of solidification in industrial processes. In the case of the conic sample the cooling rate decreases from the tip of the cone to the base. The microstructure of the cone is highly variable along the longitudinal section and this indicates a change of solidification modes due to different undercoolings. Sections have been cut at 5 mm distance from one another. Fig. 3 refers to the section of the base of the cone where the microstructure can be considered as skeletal type or vermicular. Bright zones are austenite and dark zones are ferrite as revealed by the etching. This type of morphology forms at low cooling rate and arises from the partial transformation of primary dendritic ferrite to austenite. This confirms that the alloy solidifies primarily as ferrite and then as austenite [35]. During the subsequent solid-state transformation the austenite occurring within dendrite arms of ferrite, grows into ferrite. Only the cores of the original dendrites are left with a skeleton morphology. Fig. 4 refers to a section of 5 mm away from the base and shows again a two-phase microstructure with a different morphology. It is called "lathy ferrite" and is made of several laths or plates of ferrite in an austenite matrix (same contrast as in Fig.3). Also this morphology is a result of the $\delta \rightarrow \gamma$ solid-state transformation. The austenite solidified between the secondary arms of ferrite grows not only into the ferrite arms but also into cores.

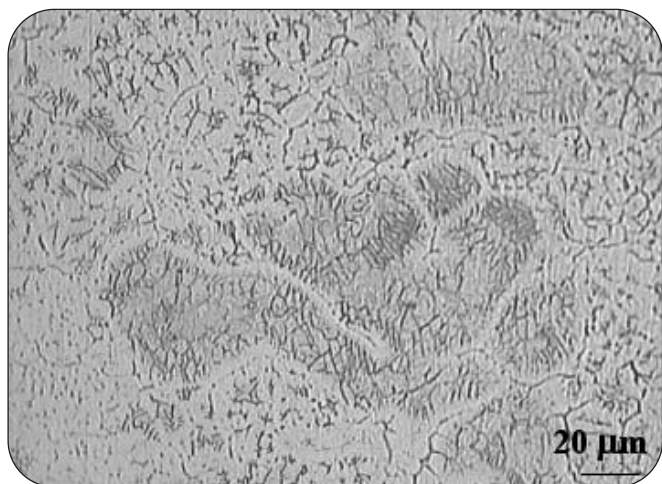


Fig. 5

Lathy ferrite microstructure in the cone of AISI 304 (tip zone).

Microstruttura con ferrite "lathy" nel cono di AISI 304 (zona in prossimità della punta).

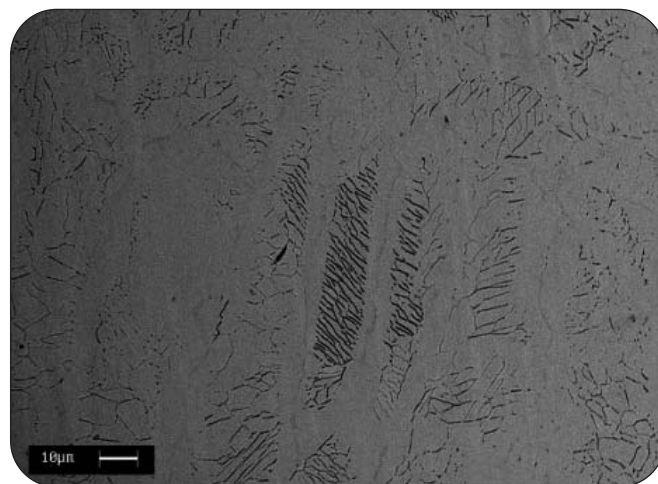


Fig. 6

Lathy ferrite microstructure. Some channel-like bright long zones are also visible. They are the result of the growth of austenite from the liquid.

Microstruttura con ferrite "lathy". Sono inoltre visibili alcune zone più chiare simili a canali che sono il risultato della crescita di austenite dal liquido.

Fig. 5 refers to a section close to the tip where an increase in the amount of the "lathy ferrite" is seen. From the Fig. 6 obtained with scanning electron microscopy the long bright zones that separate "lathy ferrite" zones are shown in detail. They are the result of the growth of austenite dendrites from the liquid after the start of primary ferrite solidification.

ANALYSIS OF THE SOLIDIFICATION MECHANISM

Another important aspect of solidification is microsegregation. It is caused by the redistribution of solute during solidification, as solute is generally rejected into the liquid. For these reasons microsegregation is a significant problem in many metallic alloy systems and it can be useful to study as the concentration of a solute varies with the velocity of the interface. To this purpose the movement of the interfaces between the phases of the system have been simulated. Such a problem is called moving boundary problem because the position of the interface is not known a priori but is the result of the solution of the diffusion problem. Moreover boundary conditions have to be formulated in order to solve the following diffusion differential equation.

$$\frac{\partial C}{\partial t} + \nabla \cdot J = 0 \quad (6)$$

where C is the concentration of the solute and J is the flux vector defined as:

$$J_k = - \sum_{j=1}^n D_{kj} \frac{\partial C_j}{\partial x} \quad (7)$$

where D_{kj} are the interdiffusion coefficients. The diffusion equation is dependent on time and its solution can be obtained only with numerical methods. In this paper, in order to analyse the mechanism of solidification for AISI 304-type steels. DICTRA (Diffusion Control

TRAnsformations) software [36] has been used. Such a software is designed for solving the diffusion problem by means of a Newton-Raphson iteration technique so as to determine the migration rate of interfaces and the phase equilibrium at interfaces.

Usually, DICTRA divides the system into cells. Cells are linked under the assumption of diffusional equilibrium and each of them contains one or more regions in which the diffusion problem is solved.

During the simulation the size of a cell is fixed while the size of a phase may grows or shrink. Two neighbouring phases are separated by a mobile interface. At the interface local equilibrium conditions are assumed while the conditions of the cell boundary are given by the user. For each phase the diffusion equation is solved by the finite difference method. The equation is numerically solved only on the points of the grid in which the region is divided. They are not fixed but their position is adjusted as a result of the simulation. The accuracy of DICTRA simulations not only depends on the accuracy of the database but also on the choice of the geometry. In our case the simulation is performed from the middle of the interdendritic region to the middle of the dendrite itself. The extent of the area corresponds to half of the interdendritic distance. In our simulation the area is about of 50 μm and the interface has been assumed to be planar. Using the composition of tab. 1 the calculations have been repeated at different temperatures, 1700 K, 1690 K, 1635 K and 1575 K. Differently from [37] the use of equivalents has been abandoned and all the solutes have been considered in the calculation.

Concentration profiles for Cr and Ni are shown in Fig. 7 and Fig. 8. In the range of temperatures between 1700 K and 1690 K, liquid phase, δ -ferrite and γ -austenite are present. This last phase appears between the liquid and the δ -ferrite and when the temperature decreases from 1700 K to 1690 K, it grows into the liquid phase and into

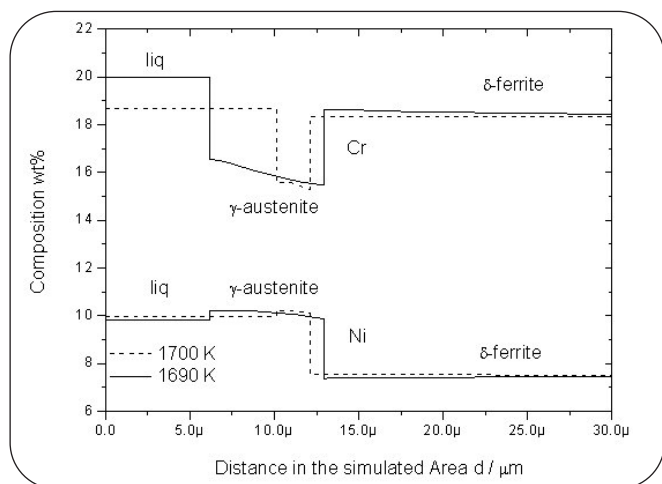


Fig. 7

Concentration profiles for Cr and Ni in δ-ferrite and in γ-austenite as a function of the simulation area at a temperature of 1700 K (dash line) and 1690 K (dot line). Austenite separates the liquid phase and the δ-ferrite.

Profili di concentrazione per il Cr e il Ni in δ-ferrite e in γ-austenite in funzione dell'area di simulazione alle temperature di 1700 K (linea tratteggiata) e 1690 K (linea a punti).

L'austenite separa la fase liquida dalla ferrite δ.

the δ-ferrite as it is demonstrated by the movement of the interfaces.

Then the liquid phase disappears and only δ-ferrite and γ-austenite are left. On cooling DICTRA predicts a movement of the γ / δ interface from the left to the right of the simulation area when the temperature decreases. This means that the austenite is growing to the detriment of ferrite.

The whole solidification mechanism has been schematically shown in Fig.9. It is in agreement with a peritectic-type mechanism.

CONCLUSION

Our study is concerned with the possibility to use modelling as a powerful tool in order to get important information about the behaviour in solidification of AISI 304-type austenitic stainless steels. Multicomponent phase selection theory and multicomponent diffusion theory have been used. Besides casting onto copper substrate techniques has been used in order to obtain variations in microstructure along the longitudinal section of the cone due to different undercoolings experimented. Microstructures obtained reproduce morphologies typical for weldings [38]. Both calculations based upon a multicomponent model of the phase selection and the microstructures found confirm that there is no δ → γ transition for the composition of the steel considered as a function of undercooling in dendritic growth. Moreover, the use of DICTRA has allowed to calculate concentration profiles for each solute giving useful information about microsegregation and confirms that the mechanism of solidification for this type of steels is peritectic-type.

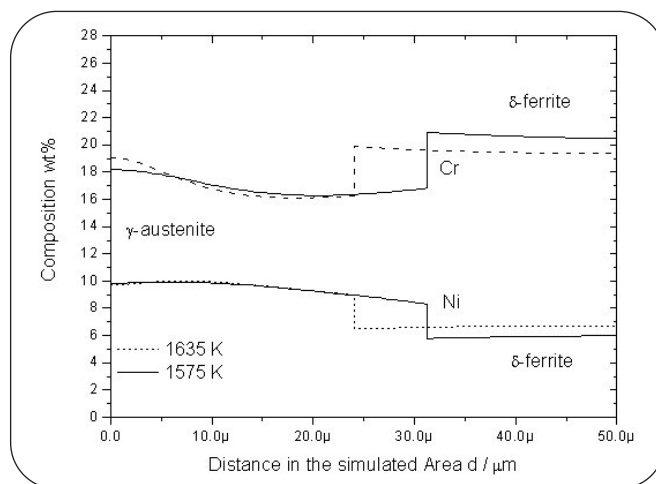


Fig. 8

Concentration profiles for Cr and Ni in δ-ferrite and in γ-austenite as a function of the simulation area at a temperature of 1635 K (dash line) and 1575 K (dot line). Austenite grows to the detriment of ferrite in agreement with the peritectic mechanism.

Profili di concentrazione per il Cr e il Ni in ferrite δ e in austenite γ in funzione dell'area di simulazione alle temperature di 1635 K (linea tratteggiata) e 1575 K (linea a punti). L'austenite cresce a spese della ferrite in accordo con il meccanismo di solidificazione peritettico.

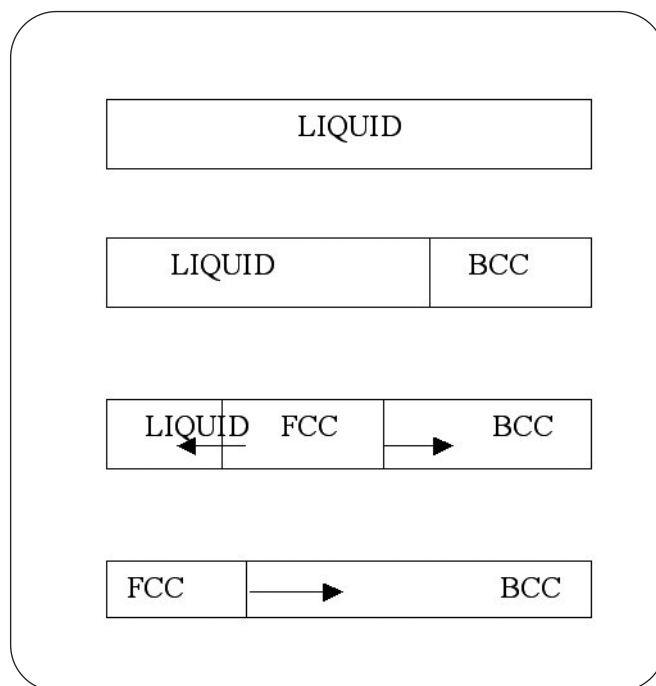


Fig. 9

Peritectic mechanism. As schematically shown above, after the nucleation of the δ-ferrite the peritectic γ-phase interacts with both δ-phase and liquid phase growing to the detriment of both phases.

Meccanismo peritettico. Come mostrato schematicamente sopra, dopo la nucleazione della ferrite δ la fase peritettica γ interagisce sia con la fase δ che con il liquido crescendo a spese di entrambe le fasi.

REFERENCES

- [1] R.D. Pehlke, Metallurgical and Materials Transaction A, 2002, 33A, p. 2252
- [2] J.D. Hunt, Acta Metall. Mater., 1991, 39, p.2117
- [3] A. Das, I. Manna, S.K. Pabi, Acta mater., 1999, 47, No. 4, p. 1379
- [4] J.D. Hunt, S.Z. Lu, Metallurgical and Materials Transaction A, 1996, 27A, p.611
- [5] T.W. Clyne, Metal Science, 1982, 16, p. 441
- [6] V.R. Voller, C.Beckermann, Metall. Mater.Trans.A., 1999, vol. 30A, p. 2183
- [7] C.Y.Wang, C.Beckermann, Mater. Sci. Eng., 1983, 171, p. 199
- [8] Y.Ueshima, S. Mizoguchi, T.Matsumiya, H.Kajioka, Metall. Trans. B, 1986, 17B, p. 845
- [9] Thermocalc A.B., SSOL database
- [10] K. Rajasekhar, C.S. Harendranath, R. Raman, S.D. Kulkarni, Material Characterization, 1997, 38, p.53
- [11] M. Bobadilla, J.Lacaze, G. Lesoult, Scandinavian Journal of Metallurgy, 1996, 25, p.2
- [12] J.A.Sarreal, G.J.Abbaschian, Metall.Trans. A, 1984, 17A, p. 2063
- [13] J.W.Elmer, S.M.Allen, T.W.Eagar, Metall. Trans. A 20A (1989) 2117
- [14] T.Umeda, T.Okane and W. Kurz, Acta mater., 1996, 44, No.10, p. 4209
- [15] O.Hunziker, M.Vandyoussefi, W.Kurz, Acta Mater.46 (18) (1998) 6325
- [16] Proceedings of the 2nd International Conference on Trends in Welding Research, Gatlinburg, TN, 14-18 May, 1989, published by ASM International
- [17] T. Volkmann, W. Loser, D. M. Herlach, Metallurgical and Materials Transactions A, Vol.28 A, pp.453-459, 1997
- [18] T. Volkmann, W. Loser, D. M. Herlach, Metallurgical and Materials Transactions A, Vol.28 A, pp.461-469, 1997
- [19] S. A. Moir, D. M. Herlach, Acta metall. Vol. 45, No. 7, pp. 2827-2837, 1997
- [20] N. Suutala, T. Takalo, T. Moisio, Metallurgical Transactions A, 1979, 10A, p. 1183
- [21] N.Suutala, T. Takalo, T. Moisio, Metallurgical Transactions A, 1980, 11A p. 717
- [22] D.Baldissin, Marcello Baricco, Livio Battezzati, Proc., 2nd International Conference Exhibition on New Developments in Metallurgical Process Technology, paper n.151, Riva del Garda, 2005, (published by Associazione Italiana di Metallurgia)
- [23] G.P. Ivantsov, Dokl. Akad. Nauk, SSSR, 1947, 58, p.567
- [24] J.S. Langer H. Muller-Krumbhaar, Acta Metall., 1978, 26, p. 1681
- [25] D. Baldissin, Phd Thesis in Science of Materials, 2006, University of Turin
- [26] J.S. Langer, H. Muller-Krumbhaar, J. Crystal Growth 1977, 42, pp. 11-14
- [27] J.S. Langer and H. Muller-Krumbhaar, Acta Metall., 1978, 26, p.1689
- [28] R.Trivedi, W.Kurz, Int. Mater. Rev. 39 (2) (1994) 49
- [29] C. B. Arnold, M. J. Aziz, M. Schwarz, D. M. Herlach, Physical Review B, 1999, 59, p. 334.
- [30] F. Spaepen, Acta Metallurgica, 1975, 23, p. 729.
- [31] Moré, J. J., "The Levenberg-Marquardt Algorithm: Implementation and Theory," Numerical Analysis, ed. G. A. Watson, Lecture Notes in Mathematics 630, Springer Verlag, 1977, p.105
- [32] S.S. Babu, J.M. Vitek, S.A. David, T. Palmer, J.W. Elmer, Proc. Symposium on the Thermodynamics, Kinetics, Characterization and Modeling of: Austenite Formation and Decomposition; Chicago; Illinois; 9-12 Nov.2003. pp. 343-352.
- [33] S. Fukumoto, W. Kurz, ISIJ International, 1999, 39, p. 1270
- [34] J.Miettinen, Metall. Mater. Trans. B 28B (1997) 281
- [35] G.K.Allan, Ironmaking and Steelmaking, 22, 6, (1995), 465-477
- [36] B. Sundman, B. Jonsson and J-O. Andersson: CAL-PHAD, 1985, 9, p.153
- [37] Daniele Baldissin, L.Battezzati, M.Rita Ridolfi, O.Tassa, Proc. 1st International Conference Super-High Strength Steels, paper n. 128, Rome, 2006, (published by Associazione Italiana di Metallurgia)
- [38] J.A. Brooks, A.W. Thompson, International Materials Review, 1991, 36, No.1 p.16

ABSTRACT

MODELLIZZAZIONE ED ESPERIMENTI DI SOLIDIFICAZIONE DI UN ACCIAIO AISI 304

Parole chiave: AISI 304, selezione di fase, sottoraffreddamento, rapida solidificazione, crescita dendritica, teoria della diffusione a molte componenti, problemi moving boundary

Uno dei più importanti processi nella Scienza dei Materiali è quello della solidificazione di metalli e leghe. Il comportamento in solidificazione di una lega così come la dimensione e la forma dei grani, la distribuzione di inclusioni, l'estensione e il numero dei difetti, le eventuali porosità del materiale o la possibile formazione di hot cracks dipendono fortemente da come l'interfaccia solido/liquido evolve nel tempo. In letteratura [1-5] sono stati fatti molti sforzi per simulare la dinamica d'interfaccia, la selezione delle fasi, la crescita peritettica e la solidificazione rapida ricorrendo a sofisticati modelli numerici che hanno permesso di trattare geometrie complesse quali quelle dendritiche.

Nella prima parte di questo lavoro è simulata la solidificazione di un acciaio AISI 304, la cui composizione è riportata in Tabella 1, utilizzando la teoria della selezione di fase estesa a sistemi a molti componenti. Scegliendo in modo opportuno i parametri termofisici del sistema (Tabella 2) con tale teoria è possibile predire quale fase, ferrite o austenite, si formi per prima in seguito al processo di solidificazione della lega dal liquido. È stato mostrato che leghe che solidificano come ferrite primaria sono più resistenti alla formazione di cricche di quelle che solidificano come austenite primaria. La velocità di raffreddamento inoltre, influenza sia il contenuto di ferrite dendritica primaria che solidifica dal liquido che il contenuto di ferrite dovuta alla trasformazione dell'austenite durante la solidificazione. Il contenuto di ferrite residua di leghe che solidificano come ferrite primaria aumenta con la velocità di raffreddamento perché ad alte velocità la trasformazione

δ - γ ha meno tempo per avvenire. Al contrario, leghe che solidificano come austenite dendritica primaria e formano ferrite come fase secondaria, mostrano un contenuto di ferrite residua che diminuisce con la velocità di raffreddamento perché durante la solidificazione ad alte velocità c'è una minore formazione di ferrite. Pertanto, una comprensione del meccanismo di solidificazione è importante per avere informazioni sulla sequenza della formazione delle fasi.

I risultati della simulazione sono riportati in Figura 2 dove la temperatura della punta dendritica, sia per la fase δ che per la fase γ , è riportata in funzione della velocità di crescita.

Per la composizione dell'acciaio e le velocità di crescita considerate, i calcoli mostrano che la temperatura della punta dendritica della fase δ è sempre più alta della temperatura dendritica della fase γ e quindi la fase δ è favorita nella solidificazione primaria per ogni velocità di crescita.

Al fine di verificare le previsioni della simulazione, nella seconda parte del lavoro sono stati effettuati degli esperimenti di solidificazione utilizzando la tecnica della colata in stampo conico con cui si ottiene un gradiente di velocità di raffreddamento tra la punta e la base del cono. Grazie a questa tecnica è stato possibile riprodurre microstrutture (Figure 3-6) usualmente ottenute in processi industriali come la saldatura. In tutti i casi, anche in prossimità della punta del cono dove le velocità di raffreddamento sono più alte, l'evidenza microstrutturale è che la fase primaria sia δ che transisce a γ per reazione nello stato solido lasciando residui dello scheletro dendritico originario.

Infine, per descrivere e verificare eventuali fenomeni di microsegregazione, nell'ultima parte del lavoro la teoria della diffusione estesa a molti componenti è stata usata nella simulazione di un problema con movimento d'interfaccia, come la solidificazione peritettica. È stato così possibile ottenere dei profili di concentrazione per il nichel e il cromo nella fase δ e nella fase γ (Figure 7 e 8) dopo la crescita peritettica tipica di questa lega (Figura 9).